Original Research Paper

Mathematics

A NEWLY ENHANCED TWO-LANE LATTICE HYDRODYNAMIC MODEL IS BEING UTILIZED TO EXPLORE THE INFLUENCE OF LANES ON JERK

Meenakshi Mehra	Department of Mathematics, Maharshi Dayanand University, Rohtak, Haryana, India
Rinku Mehra	Department of Mathematics, Jagan Nath University, Jaipur, Haryana, India
Poonam Redhu*	Department of Mathematics, Maharshi Dayanand University, Rohtak, Haryana, India *Corresponding Author

ABSTRACT This present study confronts the challenges arising from the prevalence of non- motor vehicles on two-lane roads by developing and analyzing a lattice hydrody- namic (L-H) model that incorporates jerk dynamics. The research adopts a three- phase methodology, initiating with a comprehensive examination of the system's stability using linear analysis and phase diagrams. Subsequent phases involve an in-depth exploration of the derivation of the modified Korteweg–de Vries (mKdv) equation and its solution in non-linear analysis, particularly as traffic flow ap- proaches critical points during phase transitions. To substantiate the theoretical and analytical conclusions, the study employs simulated analysis, ensuring a thorough validation of the proposed model. The assessment highlights the model's exceptional performance, especially in the con- text of two-lane roads featuring non-motor vehicles, spanning both urban and rural environments. This present research provides the traffic flow dynamics, present- ing a nuanced understanding of how non-motor vehicles impact two-lane road systems.

KEYWORDS :

1. INTRODUCTION

Traffic congestion has a direct impact on people's daily life, causing pollution, accidents, global warning and other issues due to the increasing number of auto- mobiles and modernization projects. As such, it has been imperative to perform theoretical and experimental research both to determine the underlying causes of traffic congestion in order to mitigate the issue.

Numerous mathematical models including car-following models [1, 2, 3, 4, 5], continuum models [6, 7, 8, 9, 10, 11, 12, 13] and lattice hydrodynamics models [14, 11, 15, 16, 17, 18, 19, 20, 21, 22, 23, 24, 25, 26] have been presented in order

Preprint submitted to —March 20, 2024 5 to better understand and manage the intricate mechanism underlying traffic con- gestion. Examine the characteristics of the traffic- density wave in terms of the kink-antikink- soliton, Nagatani [27] originally devised the lattice hydrodynamics model. Following that, the LH (Lattice Hydrodynamic) model has been exten- sively researched while taking into account number of factors , including impact of leading and backward sites [28, 29], effect of lane width and the anticipation of possible lane changes [30, 31, 32, 33, 34] delayed-feedback control [35]. In actual traffic scenario, abrupt vehicle acceleration and braking can result in con- siderable energy waste, increase in environmental pollution, traffic jerk and jam [36, 37, 38, 39, 40, 41, 42].

2. Proposed Model

Initaily, Nagatani [27] devloped one-lane lattice hydrodynamic model for smooth traffic flow, which is

$$\partial_t \rho_i(t) + \rho_0[q_i(t) - q_{i-1}(t)] = 0 \qquad (1)$$
$$\partial_t(q_i(t)) = \alpha[\rho_0 V(\rho_{i+1}(t)) - \rho_i v_i] \qquad (2)$$

After that, Nagatani and others also deigned new models with different factors in one-lane [43, 44, 45, 46, 47].

In this direction a one lane L-H model with jerk due to non motors vehicles developed by Redhu [48]. This research is taken by the same continuity-equation remains same while changed the flow-evolution by adding the jerk parameter.

The modified evolution equation is
$$\partial_t(q_i(t)) = \alpha[\rho_0 V(\rho_{i+1}(t)) - \rho_i v_i] + \alpha k[\rho_{i+1} v_{i+1} - \rho_i vj] - \alpha \ddot{e}[\rho_i v_i(t)$$

$$-\rho_i v_i(t - \hat{o})] \qquad (3)$$

where $q_i(t) = \tilde{n}_i(t) v_i(t)$, $\tilde{n}_i(t)$ and $v_i(t)$ are the local-density and local-velocity at j^{th} site on the two-dimensional lattice at time t, respectively. Here $\tilde{n}_0$, $\alpha = 1/\hat{o}$, $\ddot{e}$ and k are the average density, the driver's sensitivity, coefficient of jerk and coefficient of traffic flux respectively.

The following equation is of optimal velocity function:j
$$V(\rho_j(t)) = \frac{V_{max}}{2}\left[\tanh\frac{1}{\rho_j} - \frac{1}{\rho_c} + \tanh\frac{1}{\rho_c}\right] \qquad (4)$$

where V_{max} and $\tilde{n}_c$ denote the maximal-velocity and safety critical density respec- tively.

It is well known that complex traffic congestion in urban areas is caused by non-motor vehicles suddenly accelerating and decelerating considered the impact of traffic jerk when developing a car-following traffic flow model and explaining how it affected jamming transitions. The micro-level analysis of the traffic jerk parameter indicates that non-motor vehicle motion irregularities exacerbate traffic jams, hence the traffic jerk parameter is crucial to understand traffic flow theory. However, it's also discovered that the flux differential effect is crucial for keeping the gridlock in place, which is related to non-motor vehicle motion. The temporal dynamics of the vehicle flow are represented by the jerk parameter profile and more non-motor vehicles on the road typically result in traffic congestion and flow instability. Furthermore, many researchers extended the one-lane model into two-lane model with different factors. Due to more traffic in one lane, the jam will increase. So, vehicles will need a second lane to get out of the jam and perform the better flow.

As a single lane fails to adequately depict the lane-changing dynamics observed in actual traffic scenarios. The lane change rule for two-lane is as follows:

In the event that the density on lane L2 surpasses that of lane L1 at location j-1, a seamless flow is achieved by directing vehicles from lane L2 to lane L1 at site j. Similar for lane change L1 to L2 lane. This is accurately reflecting the real-world traffic phenomena.

In urban and rural areas, roads are jammed due to irregular motion of non- motorized vehicles. For the first time Redhu

checked the effect of traffic jerk on one-lane [48]. But,there are also two lane or multi lane roads where jam is due to acceleration or deceleration of non motor vehicles.

The proposed model depends upon two-lane LH model with Jerk parameter. The modified continuity equation is

$$\partial_t \rho_i(t) + \rho_0[q_i(t) - q_{i-1}(t)] = \gamma|\rho_0^2[V'(\rho_0)|\rho_{j+1} - 2\rho_j + \rho_{j-1}]$$ (5)

After removing velocity vj from Eqs. (3) and (5), density equation obtained as

$$\rho_i(t + 2\tau) - \rho_i(t + \tau) + \tau\rho^2[V(a\rho_{j+1}(t)) - V(a\rho_j(t))]$$
$$+ k[\tau\gamma|\rho_0^2[V'(\rho_0)(\rho_{j+2} - 3\rho_{j+1} + 3\rho_j - \rho_{j-1}) - \rho_{j+1}(t+\tau) + \rho_j(t+\tau)$$
$$+ \rho_{j+1}(t) - \rho_j(t) + \rho_j(t - \tau)(0)) - \lambda\gamma|\rho_0^2[V'(\rho_0)(\rho_{j+1} - 2\rho_j$$
$$+ \rho_{j+1}(t - \tau) + 2\rho_{j+1}(t - \tau)) - \rho_i(t + \tau) + 2\rho_i(t) - \rho_i(t - \tau)] = 0$$ (6)

where k is anticipation-coefficient of flux-difference and λ is jerk coefficient as above and ɣ is lane changing coefficient. When ɣ=0 it become basic model [48] for jerk effect on one lane and when k and ɣ both zero then it become Nagatani one-lane model. In the proposed model $k =/ 0$, ɣ$/= 0$ and λ 0.

3. Linear analysis
To investigate the linear-stability of the traffic jerk on effect of two-lane. The traffic-density and optimal-velocity under uniform conditions are taken as $\tilde{n}_0$ and $V(\tilde{n}_0)$, respectively. Let the steady state solution for homogeneous traffic flow's is following

$$\rho_i(t) = \rho_0$$ (7)

$$v_i(t) = V(\rho_0)$$ (8)

Let $y_j(t)$ be a small perturbation to the steady-state density on site-j. Then

$$\rho_i(t) = \rho_0 + y_i(t)$$ (9)
$$V(\rho_j(t)) = V(\rho_0) + V'(\rho_0)y_j(t),$$ (10)

Substituting $\rho_i(t) = \rho_0 + y_i(t)$ into Eq.6, then

$$y_1(t + 2\tau) - y_1(t + \tau) + \tau\rho_0^2 V'(\rho_0)[y_{j+1}(t) - y_j(t)] + k[(\tau\gamma|\rho_0^2 V'(\rho_0))(y_{j+2}(t)$$
$$- 3y_{j+1}(t) + 3y_j(t) - y_{j-1}(t))(-y_{j+1}(t+\tau) + y_j(t+\tau) + y_{j+1}(t)$$
$$- y_j(t))] - \lambda[\tau\gamma|\rho_0^2 V'(\rho_0))(y_{j+1}(t) - 2y_j(t) + y_{j-1}(t) - y_{j+1}(t-\tau)$$
$$+ 2y_j(t - \tau) - y_{j-1}(t-\tau))(-y_j(t + \tau) + 2y_j(t) + y_{j-1}(t - \tau))] = 0$$ (11)

where $V(\rho_0) = \frac{dV(\rho)}{d\rho}$ at $\rho = \rho_0$.
Putting $y_j(t) = e^{ikj - zt}$ in Eq. (11), obtained that

$$e^{2z\tau} - e^{z\tau} + \tau\rho_0^2 V'(\rho_0)[e^{ik} - 1] + k[\tau\gamma|\rho^2[(V'(\rho_0))(e^{2ik} - 3e^{ik} + 3 - e^{-ik})$$
$$- e^{ik+z\tau} + e^{z\tau} + e^{ik} - 1) - \lambda\tau(\gamma|\rho^2[V'(\rho_0))(e^{ik} - 2 + e^{-ik} - e^{-ik-z\tau} + 2e^{-z\tau}$$
$$- e^{-ik-z\tau}) - e^{-z\tau} + 2 - e^{-z\tau}]$$
$$= \rho_0^2[V'(\rho_0)|[e^{ik+z\tau} - 2e^{-z\tau} + e^{-ik+z\tau}]$$ (12)

After substituting $z = z_1(ik) + z_2(ik)^2...$ into Eq. (12), got that On comparing the coefficients of ik and $(ik)^2$, obtained that

$$z_1 = -\rho_0^2 V'(\rho_0)$$ (13)

$$z_2 = -\frac{3}{2}\tau z_1^2 + \frac{1}{2}z_1 + \lambda z^2\tau - kz_1 + \gamma z_1 \quad 2005/06/28ver : 1.3su$$

When $z_2 < 0$, then it become unstable for uniform steady-state for long-wavelength waves. Thus, the neutral stability condition is given by

$$\tau = \frac{-(1 + 2(k + \gamma))}{(3 + 2\lambda)\rho_0^2 V'(\rho_0)}$$ (15)

Eq15 Illustrates the importance of the lane coefficient (ɣ) and the jerk param- eter in playing a pivotal role in stabilizing traffic flow.

In fig 1, the amplitude of the neutral stability curve for the value λ=0, k=0.1 and λ =0.2 significantly higher to the proposed model for ɣ=0.2, k=0.1 and λ=0.2. This clearly

illustrates that the stability zone of the suggested model much out- performs that of the Redhu model, demonstrating the proposed model's superior performance.
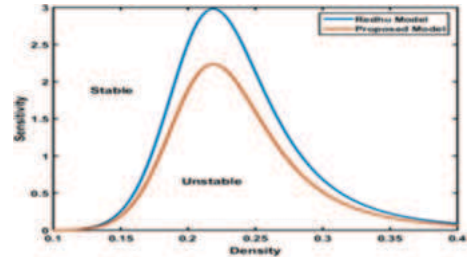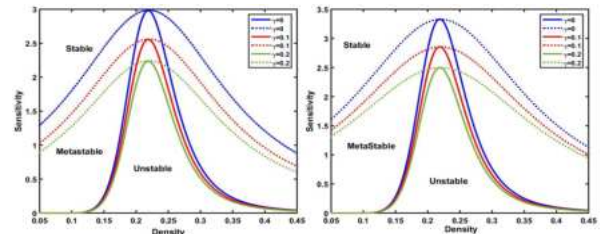

Figure 1: Phase diagram in density-sensitivity with comparison of Redhu model

(a)   **(b)**
Figure 2: Phase diagram in density-sensitivity for fixed value of k and different values of $\tilde{a}$ with
(a) λ = 0.2 **(b)** λ = 0.4

4. Nonlinear
A reductive perturbation strategy is used for a nonlinear stability study of the proposed model at the critical point (ρ_c, α_c).At this scale, the utilization of long- wavelength expansion is employed to elucidate the gradual shifting behavior near the critical point and establish slow scales for spatial and temporal variables.

The slow-variables X and T are listed below. For a small positive parameter Ɛ, the slow variables X and T are defined as

$$X = \tilde{a}(j + bt), T = \varepsilon^3 t$$ (16)

where b is constant to be determined. Let ρ_j satisfy the following equation:
$$\rho_j(t) = \rho_c + \varepsilon R(X, T)$$ (17)

By expanding Eq. (6) upto the fifth order of Ɛ with the use of Eqs. (16) and (17), following nonlinear PDE(partial differential equation) is obtained: To solve the above equation using

$V = \frac{dV(\rho)}{d\rho}$ and $V'' = \frac{d^2V(\rho)}{d\rho^2}$ at $\rho = \rho_c$.

In the neighborhood of critical point T_c, define $T = T_c(1 + []^2)$ and choosing $b = -\rho_c^2 V'(\rho_c)$.

Eliminating second and third order terms of $\tilde{a}$ into Eq. (6), obtained that

$$\varepsilon^4(\partial_T R - g_1\partial^3 R + g_2\partial_X R^3) + \varepsilon^5(g_3\partial^2 R + g_4\partial^4 R + g_5\partial^2 R^3) = 0$$ (18)

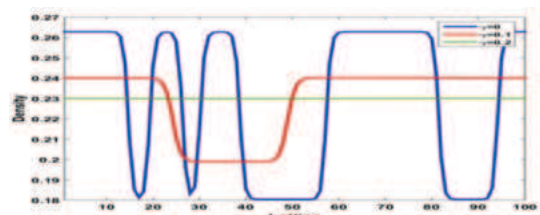**Figure 3:** Density profiles at time t=10300 and λ = 0.2 when α = 2.4 and ɣ vary

(a)

(b)

©

Figure 6: Spatiotemporal evolutions of density at time t=10300 when α = 2.6 when (α)γ= 0(b) γ= 0.1 and (c) γ = 0.2
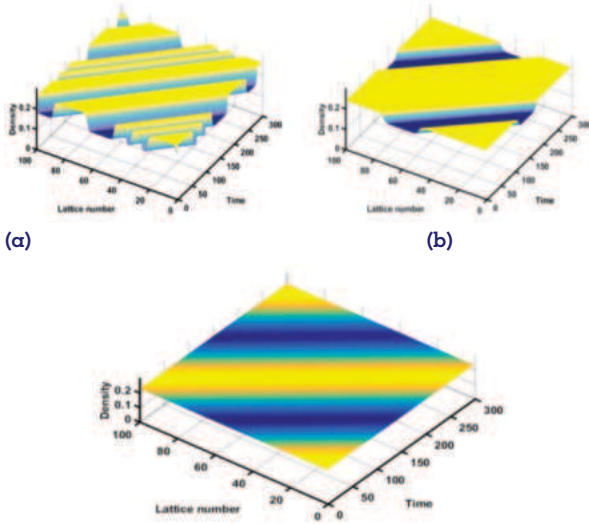

©

Figure 4: Spatiotemporal evolutions of density at time t=10300 when λ =0.2 and α=2.4, when (α)γ = 0.0(b)γ = 0.1 and (c)γ= 0.2
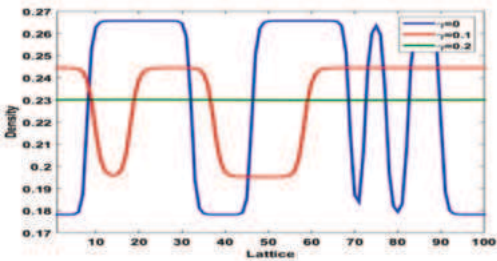

Figure 5: Density profiles at time t=10300 when α=2.6, λ = 0, 4 and γ-vary

where g_1, g_2, g_3, g_4 and g_5 as follows

$$g_1 = \frac{7}{6}b^3T^2 - \frac{\rho^2 v'}{c} + \lambda\gamma\rho^2 v'bT + k\gamma\rho^2 v' - \frac{kb}{2} - \gamma\rho^2 v'bT \quad (19)$$

$$g_2 = \frac{\rho_i^2 v'''}{6} \quad (20)$$

$$g_3 = \frac{3}{2}b^2\rho^2 v' + \lambda b^2 T^2 \quad (21)$$

$$g_4 = \frac{5}{8}b^2T^2 + \frac{\rho^2 v'}{c}\left(\frac{c}{40} + \frac{bT^3}{bKO\cdot l_c + 40'l_c^2} + \frac{h^4T^4}{h_c^2T^2}\right) + \left(R\frac{\rho^2 v' v}{\gamma\mu^2 v}\right) \quad (22)$$

$$+\left(\frac{}{24}\right) - \gamma\rho_c^2 v' - \frac{c}{2} + \frac{c}{12} \quad (23)$$

$$+[3bT_c + 2\lambda bT_c - k]g_1 \quad 2005/06/28ver : 1.3su$$

$$g_5 = \frac{\rho_c^2 v'''}{12} - (3bT_c + 2\lambda bT_c)g_2 \quad (25)$$

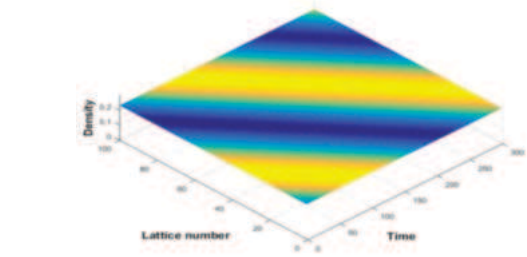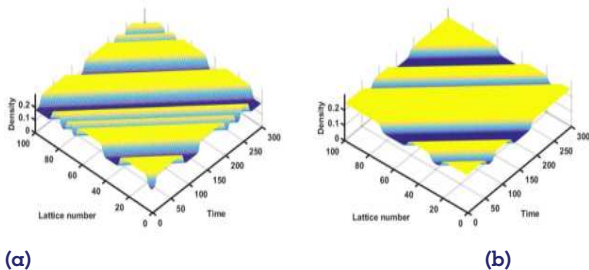In order to derive the standard mKdV equation, following transformations have been in used in Eq.

(a)

(b)

$$\partial_T R' - \partial_{\hat{X}}^3 R' + \partial_X R^3 + \epsilon M[R] = 0, \quad (26)$$

where $M[R] = -\frac{1}{g_1}\left[g_3\partial^2 R' + \frac{\mu'g_5^2}{g_2}\partial^2 R^3 + g_4\partial^4 R'\right]$.

To left the $O(\epsilon)$terms in Eq. (26).The standard modified Korteweg-de Vries (mKdV) equation is derived, yielding the sought-after kink-soliton solution.

$$R'_0(X, T') = \sqrt{c}\tanh\sqrt{\frac{c}{2}}(X - cT'). \quad (27)$$

$$(R', M[R']) \equiv \int_{\infty}^{\prime\infty} dXR' M[R'] = 0, \quad (28)$$

$$c = \frac{5g_2 g_3}{2g_2 g_4 - 3g_1 g_5}. \quad (29)$$

Hence, the kink-antikink solution is given by

$$\rho_j(t) = \rho_0 + \epsilon\sqrt{\frac{g_1 c}{g_2}}\tanh\sqrt{\frac{c}{2}}(X - cg_cT'), \quad (30)$$

with $\epsilon^2 = \frac{T}{T_c} - 1$ and the Height A of the solution is

$$A = \frac{5}{g_2}\sqrt{g_1^2\epsilon^2 c}, \quad (31)$$

Figure2(α) and 2(b) represent the phase diagram of density and sensitivity.The dotted curves in figure2(α) and 2(b)

Corresponding to nonlinear analysis, these are referred to as coexisting curves—and derived the mKdV equation. The kink–antikink solution symbolizes the coexisting- phase, encompassing both the freely-moving and congested phases, and can be characterized by $\rho_j = \rho_c + A$ and $\rho_j = \rho_c$ A respectively in the phase space (ρ, α). For a particular case, when γ= 0 the results become similar to those found by the Redhu proposed model [48].Figure2(α) and 2(b)

The complete region diveded in three phages due to the coexisting and neutral stability curves the region above the coexisting-curve is stable, the region un- der the neutral-stability curve is unstable, and the region between the coexisting and neutral-stability curves is meta-stable. According to the figure2(α) and 2(b), stable-region increases with increasing $\tilde{\alpha}$, for $\ddot{e}$ =0.2 and 0.4. Without loss of gen- erality and the sake of definiteness incorporate the two-lane lattice hydrodynamic traffic flow model effect with traffic jerk in studying the impact on congestion due to non-motor vehicles.

5. Numerical Simulation

In this phage theoretical results is carried out for the new model with periodic- boundary conditions. The initial conditions are given as follows:

$$\rho_j(0) = \rho_j(1) = \begin{cases} \rho_0, & \text{if } j \neq \frac{L}{2}, \frac{L}{2}+1 \\ \rho_0 - \sigma, & \text{if } j = \frac{L}{2} \\ \sigma \text{ if } j = \frac{L}{2}+1 \end{cases}$$

Where σ represents the initial disturbance, and L is the total number of sites, set to 100, with other parameters configured as follows: σ = 0.1, $T = \frac{1}{-}$. For computational purposes, the maximal velocity and critical density are defined as 2 and 0.23, respectively.

Figure 3 illustrates the simulation results of density-evolution after 10^4 time steps for varying values of γ when k = 0.1 and λ = 0.2. Notably, in Figure 4(c), the initial perturbation diminishes for γ = 0.2 within the stable region, resulting in a uniform traffic flow. As ã decreases to 0.1, the uniform flow transitions into a congested flow with kink–antikink-soliton density-waves in the "unstable" region, propagating backward over time, as depicted in Figure 4(b). Furthermore, with a decrease to γ = 0.0, the number and height of stop-and-go waves increase, leading to congestion, as evident in Figure 4(a). The height of density-waves decreases with an increase in the value of ã for k = 0.1 and λ = 0.2, expanding the stable region. Hence, the presence of traffic jerk in the two-lane traffic model contributes to road congestion.

Similarly, in Figure 6©, the simulation results for density-evolution after 10^4 time steps with different γ values are shown for k = 0.1 and λ = 0.4. As γ decreases to 0.1, the uniform flow transforms into a congested flow with kink–antikink- soliton density-waves in the unstable-region, as illustrated in Figure 6(b). Further reduction in γ to 0.0 intensifies the number and height of stop-and-go waves, lead- ing to congestion, as shown in Figure 6(c). Figures 5 and 3 demonstrate that the height of density-waves goes to be decreases with an increase of γ for k = 0.1, λ = 0.4, and λ = 0.2, resulting in a reduction of the unstable region. Therefore, the presence of traffic jerk in the two-lane traffic model contributes to road congestion.

Similar patterns emerge when the proposed model increases the coefficient of flux, k = 0.2 and 0.3, respectively. In the stable-region, traffic-flow becomes uniform, and the initial perturbation diminishes, while in the unstable-region, per- turbation transforms into kink–antikink structures.

Comparing results for lower and higher for the values γ, it is conclude that the impact of two-lane traffic jerk aids in mitigating traffic congestion induced by the motion of non-motor vehicles. This study highlights the crucial role of two-lane traffic jerk in traffic flow theory, particularly in the flux difference LH model, suggesting its consideration in traffic flow modeling studies.

6. CONCLUSION
The present model is built upon a two-lane lattice hydrodynamic system. Through the analysis of this model, for increasing the lane coefficient in a two-lane system, while maintaining a constant anticipation of traffic flux and jerk coefficient, leads to an expansion of the stable-region. The findings indicate that the inclusion of a two-lane parameter contributes to alleviating traffic-congestion for various jerk scenarios. The simulation-results go with theoretical expectations.

Consequently, it is reasonable to assert that both traffic jerk and two-lane pa- rameters play pivotal roles in stabilizing traffic flow.so this should be considera- tion when developing traffic flow models and it promise for giving the valuable-insights that can be applied to address analogous challenges, especially in the enhancement of multi-lane traffic systems.

Data Availability Statement
There are no related data with this manuscript, or the data will not be submit- ted.

REFERENCES

[1] X. Wang, J. Zhang, H. Li, Z. He, A mixed traffic car-following behavior model, Physica A: Statistical Mechanics and its Applications 632 (2023) 129299.
[2] Z. Wang, Y. Shi, W. Tong, Z. Gu, Q. Cheng, Car-following models for human-driven vehicles and autonomous vehicles: A systematic review, Journal of Transportation Engineering, Part A: Systems 149 (8) (2023) 04023075.
[3] X. Chen, M. Zhu, K. Chen, P. Wang, H. Lu, H. Zhong, X. Han, X. Wang, Y. Wang, Follownet: a comprehensive benchmark for car-following behavior modeling, Scientific data 10 (1) (2023) 828.
[4] W. Du, Y. Li, J. Zhang, Stability control of a two-lane car-following model based on cluster synchronization of complex network, Optimal Control Applications and Methods (2023).
[5] X. Zhang, Z. Shi, J. Chen, et al., A bi-directional visual angle car-following model considering collision sensitivity, Physica A: Statistical Mechanics and its Applications 609 (2023) 128326.
[6] L. Yu, A new continuum traffic flow model with two delays, Physica A: Statistical Mechanics and Its Applications 520 (2020) 123757.
[7] R. Mohan, G. Ramadurai, Heterogeneous traffic flow modelling using second-order macroscopic continuum model, Physics Letters A 381 (3) (2017) 115–123.
[8] A. K. Gupta, P. Redhu, Analyses of the driver's anticipation effect in a new lattice hydrodynamic traffic flow model with passing, Nonlinear Dynamics 76 (2014) 1001–1011.
[9] Y. Jiang, S. Wong, H. Ho, P. Zhang, R. Liu, A. Sumalee, A dynamic traf- fic assignment model for a continuum transportation system, Transportation Research Part B: Methodological 45 (2) (2011) 343–363.
[10] A. K. Gupta, S. Sharma, Nonlinear analysis of traffic jams in an anisotropic continuum model, Chinese Physics B 19 (11) (2010) 110503.
[11] J. Besson, Continuum models of ductile fracture: a review, International Journal of Damage Mechanics 19 (1) (2010) 3–52.
[12] C. Wagner, C. Hoffmann, R. Sollacher, J. Wagenhuber, B. Schu¨rmann, Second-order continuum traffic flow model, Physical Review E 54 (5) (1996) 5073.
[13] S. T. Fiske, M. Lin, S. L. Neuberg, The continuum model: Ten years later, Social cognition (2018) 41–75.
[14] M. Bando, K. Hasebe, A. Nakayama, A. Shibata, Y. Sugiyama, Dynami- cal model of traffic congestion and numerical simulation, Physical review E 51 (2) (1995) 1035.
[15] G. Peng, X. Cai, B. Cao, C. Liu, Non-lane-based lattice hydrodynamic model of traffic flow considering the lateral effects of the lane width, Physics Letters A 375 (30-31) (2011) 2823–2827.
[16] C. Zhu, S. Zhong, S. Ma, Two-lane lattice hydrodynamic model considering the empirical lane-changing rate, Communications in Nonlinear Science and Numerical Simulation 73 (2019) 229–243.
[17] T. Wang, R. Cheng, H. Ge, Analysis of a novel two-lane lattice hydro- dynamic model considering the empirical lane changing rate and the self-stabilization effect, IEEE Access 7 (2019) 174725–174733.
[18] T. Wang, R. Cheng, H. Ge, An extended two-lane lattice hydrodynamic model for traffic flow on curved road with passing, Physica A: Statistical Mechanics and Its Applications 533 (2019) 121915.
[19] T. Wang, Z. Gao, J. Zhang, X. Zhao, A new lattice hydrodynamic model for two-lane traffic with the consideration of density difference effect, Nonlinear Dynamics 75 (2014) 27–34.
[20] C. Zhai, W. Wu, Stability analysis of two-lane lattice hydrodynamic model considering lane-changing and memorial effects, Modern Physics Letters B 32 (20) (2018) 1850233.
[21] C. Zhai, W. Wu, Y. Xiao, The jamming transition of multi-lane lattice hydro-dynamic model with passing effect, Chaos, Solitons & Fractals 171 (2023) 113515.
[22] X. Li, C. Jin, G. Peng, The impact of the density delay on the traffic evolu- tion process in lattice hydrodynamic model under lane change on two lanes, Europhysics Letters 141 (3) (2023) 33002.
[23] Y. Li, T. Zhou, G. Peng, Incorporating the traffic interruption probability effect during evolution process in two-lane lattice hydrodynamic model, International Journal of Modern Physics C 34 (03) (2023) 2350035.
[24] T. Li, F. Hui, C. Liu, X. Zhao, A. J. Khattak, Analysis of v2v messages for car-following behavior with the traffic jerk effect, Journal of Advanced Transportation 2020 (2020) 1–11.
[25] Z. Cong, W. Wu, Macro autonomous traffic flow model with traffic jerk and downstream vehicle information, Engineering Computations 38 (10) (2021) 4066–4090.
[26] H. Qi, Are current microscopic traffic models capable of generating jerk pro-file consistent with real world observations?, International Journal of Trans-portation Science and Technology (2023).
[27] T. Nagatani, Modified kdv equation for jamming transition in the contin- uum models of traffic, Physica A: Statistical Mechanics and Its Applications 261 (3-4) (1998) 599–607.
[28] G. Peng, W. Lu, H. He, Impact of the traffic interruption probability of op- timal current on traffic congestion in lattice model, Physica A: Statistical Mechanics and Its Applications 425 (2015) 27–33.
[29] P. Redhu, A. K. Gupta, Effect of forward looking sites on a multi-phase lattice hydrodynamic model, Physica A: Statistical Mechanics and its Appli- cations 445 (2016) 150–160.
[30] H. Ge, R. Cheng, The "backward looking" effect in the lattice hydrody- namic model, Physica A: Statistical Mechanics and Its Applications 387 (28) (2008) 6952–6958.
[31] G. Peng, X. Cai, C. Liu, M. Tuo, A new lattice model of traffic flow with the anticipation effect of potential lane changing, Physics Letters A 376 (4) (2012) 447–451.
[32] G. Peng, C. Luo, H. Zhao, H. Tan, Jamming transition in two-lane lattice model integrating the deception attacks on influx during the lane-changing process under vehicle to everything environment, Chaos, Solitons & Fractals 176 (2023) 114176.
[33] Y. He, J. Feng, K. Wei, J. Cao, S. Chen, Y. Wan, Modeling and simula- tion of lane-changing and collision avoiding autonomous vehicles on super-highways, Physica A: Statistical Mechanics and its Applications 609 (2023) 128328.

[34] G. Ma, K. Li, H. Sun, Modeling and simulation of traffic flow based on memory effect and driver characteristics, Chinese Journal of Physics 81 (2023) 144–154.

[35] Y. J. Meng, Jingwei, M. Xu, Stochastic dynamics of a discrete-time car-following model and its time-delayed feedback control, Physica A:Statistical Mechanics and its Applications 610 (2023) 128407.

[36] P. Fernandes, R. Toma´s, E. Ferreira, B. Bahmankhah, M. Coelho, Driving aggressiveness in hybrid electric vehicles: Assessing the impact of driving volatility on emission rates, Applied Energy 284 (2021) 116250.

[37] D. C. Selvaraj, S. Hegde, N. Amati, F. Deflorio, C. F. Chiasserini, An ml- aided reinforcement learning approach for challenging vehicle maneuvers, IEEE Transactions on Intelligent Vehicles 8 (2) (2022) 1686–1698.

[38] M. M. Ahmed, M. N. Khan, A. Das, S. E. Dadvar, Global lessons learned from naturalistic driving studies to advance traffic safety and operation re- search: A systematic review, Accident Analysis & Prevention 167 (2022) 106568.

[39] Y.-c. Zhang, Y. Xue, Y. Shi, Y. Guo, F.-p. Wei, Congested traffic patterns of two-lane lattice hydrodynamic model with partial reduced lane, Physica A: Statistical Mechanics and its Applications 502 (2018) 135–147.

[40] B. Meng, J. Yuan, S. Li, Two-lane lattice hydrodynamic modeling at sag sections with the empirical lane-changing rate, IEEE Access (2023).

[41] H.-T. Zhao, H.-Z. Li, H. Qin, L.-H. Zheng, Two-lane mixed traffic flow model considering lane changing, Journal of Computational Science 61 (2022) 101635.

[42] H. Liu, R. Cheng, H. Ge, A novel two-lane lattice hydrodynamic model on a gradient road considering heterogeneous traffic flow, Modern Physics Letters B 35 (20) (2021) 2150340.

[43] Y. Zhang, M. Zhao, D. Sun, S. hui Wang, S. Huang, D. Chen, Analysis of mixed traffic with connected and non-connected vehicles based on lattice hydrodynamic model, Communications in Nonlinear Science and Numerical Simulation 94 (2021) 105541.

[44] L. Huang, S.-N. Zhang, S.-B. Li, F.-Y. Cui, J. Zhang, T. Wang, Phase transi- tion of traffic congestion in lattice hydrodynamic model: Modeling, calibra- tion and validation, Modern Physics Letters B (2023) 2450012.

[45] Q. Peng, H. Zhao, The optimal estimation of delayed flux effect on traf- fic stability in lattice hydrodynamic model, International Journal of Modern Physics C (2023) 2350161.

[46] J. Zhou, Z.-K. Shi, C.-P. Wang, Lattice hydrodynamic model for two-lane traffic flow on curved road, Nonlinear Dynamics 85 (2016) 1423–1443.

[47] T. Wang, J. Zhang, Z. Gao, W. Zhang, S. Li, Congested traffic patterns of two-lane lattice hydrodynamic model with on-ramp, Nonlinear Dynamics 88 (2017) 1345–1359.

[48] P. Redhu, V. Siwach, An extended lattice model accounting for traffic jerk., Physica A:Statistical Mechanics and its Applications 492 (2018) 1473–1480.